

CONF-2405231--5

HISTORICAL PERSPECTIVE OF THE RELATION BETWEEN IBA AND VMI
AT THE MAGIC LIMIT: TWO OPPOSING VIEWS

NOTICE

PORTIONS OF THIS REPORT ARE ILLEGIBLE.

has been reproduced from the best available
copy to permit the broadest possible avail-
ability.

G. Scharff-Goldhaber

510A, Brookhaven National Laboratory
Upton, New York 11973
USA

BNL--35109

DE84 016441

ABSTRACT

The two-parameter rotational VMI equations ascribe the observed abrupt change in yrast bands at the magic limit to a first order phase transition. In contrast, two three-parameter anharmonic vibrator models recently suggested yield two limits of validity, neither of which is supported by data.

The two-parameter VMI equations^{1,2,3)}

$$E_J = \frac{C}{2}(\mathcal{J} - \mathcal{J}_0)^2 + \frac{J(J+1)}{2\mathcal{J}} \quad (1)$$

$$\left. \frac{\delta E}{\delta \mathcal{J}} \right|_J = 0 \quad (2)$$

leading to a cubic equation for \mathcal{J} :

$$\mathcal{J}^3 - \mathcal{J}_0 \mathcal{J}^2 = \frac{J(J+1)}{2C} \quad (3)$$

evolved from C. Mallmann's* observation⁴⁾ that the ratios R_6 and R_8 (where $R_J = \frac{E_J}{E_2}$), if plotted vs. R_4 , lie on universal curves. This

observation implies that one and the same mechanism underlies the yrast bands of all even-even nuclei. The measured quantities needed for the determination of the parameters C and \mathcal{J}_0 are E_2 and R_4 .

*Mallmann did not distinguish between bands of non-magic and magic nuclei, because the data available to him were very limited and imprecise.

MASTER

E_2 , the energy of the lowest 2^+ state, plays the role of a scale factor, which depends on the size of the nucleus as well as on the interactions of its extra-shell neutron and proton pairs. The empirical function $E_2(Z,N)$ plays the role of the "Stone of Rosetta" for the understanding of collective nuclear motions, while $R_4(Z,N)$, the basic VMI variable, measures nuclear deformation.

In contrast to the rotational interpretation represented by the VMI equations, A. Klein and his associates⁵⁾ attempted to describe the ratios of yrast band energies by an anharmonic vibrator model, which yields:

$$E = aJ + kJ(J + 1). \quad (4)$$

This expression agrees with the previously reported empirical "Ejiri formula,"⁶⁾ from which follows:

$$R_J = \frac{J(J - 2)}{8} R_4 - \frac{J(J - 4)}{4}. \quad (5)$$

Fig. 1 (taken from ref. 5) presents R_8 vs. R_4 : curve a corresponds to the anharmonic vibrator (eq. 5); curve c is deduced from VMI (eqs. 1 and 3) and curve b is given by the Bohr-Mottelson two-term expansion in $J(J + 1)$. Later, it was found that curve a also agrees with values for the 3 subgroups of IBA I. Clearly, curve c represents the data best.

The idea of studying the applicability of the VMI equations for negative values of \mathcal{J}_0 was suggested by inspection of the variation of the parameter \mathcal{J}_0 (Fig. 2). From the striking sharp decline of \mathcal{J}_0 as the neutron number decreases from $N = 90$ toward $N = 82$, it appears that below $N = 84$ or even 86, \mathcal{J}_0 will descend below the $\mathcal{J}_0 = 0$ plane. On the other hand, no such behavior occurs at the high N side of the rare earths region as ^{208}Pb is approached.

The extension to negative values of \mathcal{J}_0 ⁷⁾, which included a number of nuclei approaching $N = 82$ from below and $N = 50$ from above, led indeed to excellent agreement with the data (Fig. 3). In contrast to Mallmann's notion, a lower limit of validity of VMI is reached at $\mathcal{J}_0 \rightarrow -\infty$, where $R_4 = 1.82$ and $E \propto [J(J + 1)]^{1/2}$. This is the closed shell limit, representing a first order phase transition⁹⁾ at

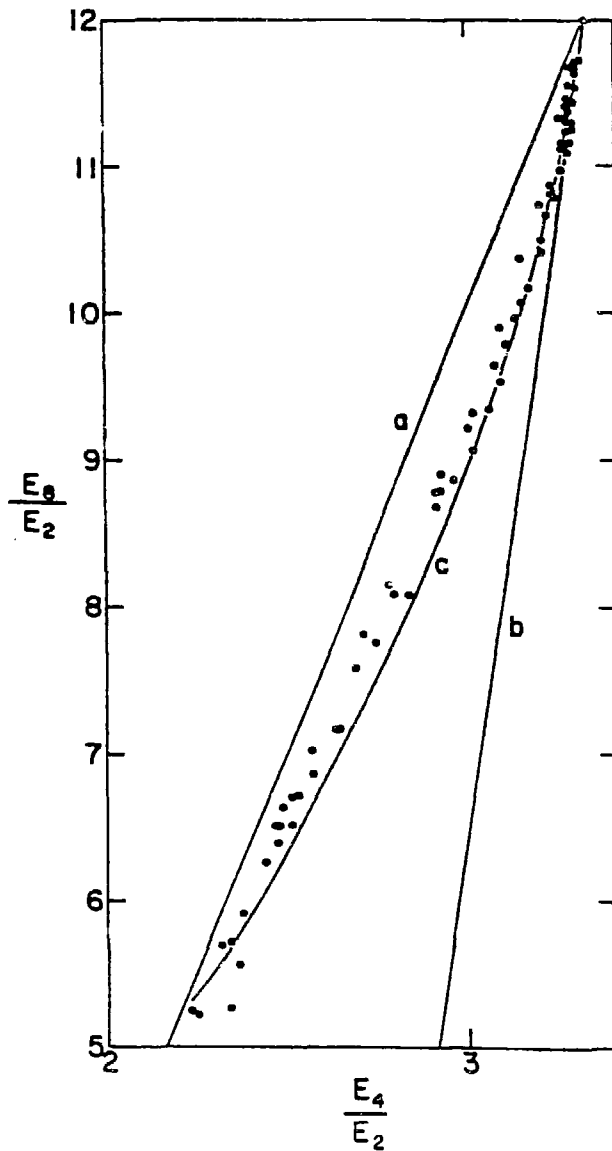


Fig. 1. E_8/E_2 plotted vs. E_4/E_2 . The solid curves correspond to predictions from a) the Ejiri formula $R_J = 1/8 J(J - 2)R_4 - 1/4 J(J - 4)$, which is identical with the prediction from the anharmonic vibrator model; b) the Bohr-Mottelson two-term expansion in $J(J + 1)$; and c) the VMI equations. The figure is reproduced from ref. 5.

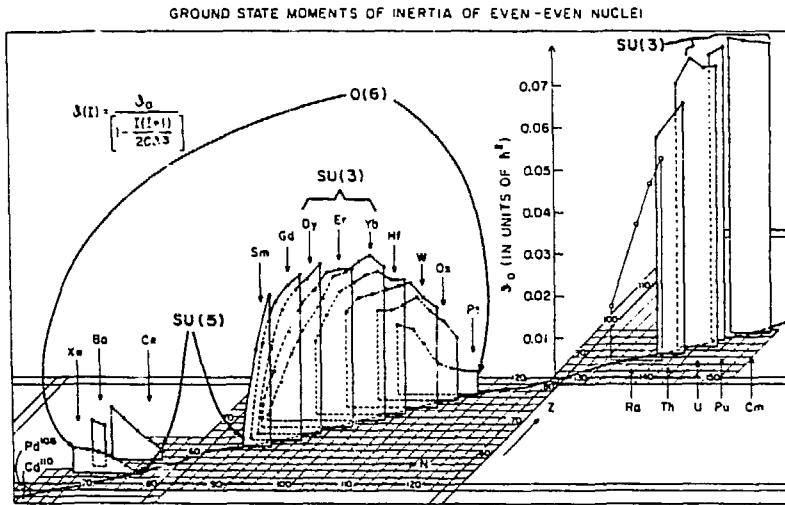


Fig. 2. Three-dimensional diagram of J_0 (computed from eqs. 1 and 3) vs. N and Z . This figure was first published in ref. 1. More recent interpretations⁸⁾ by IBA I subgroups are indicated in this figure.

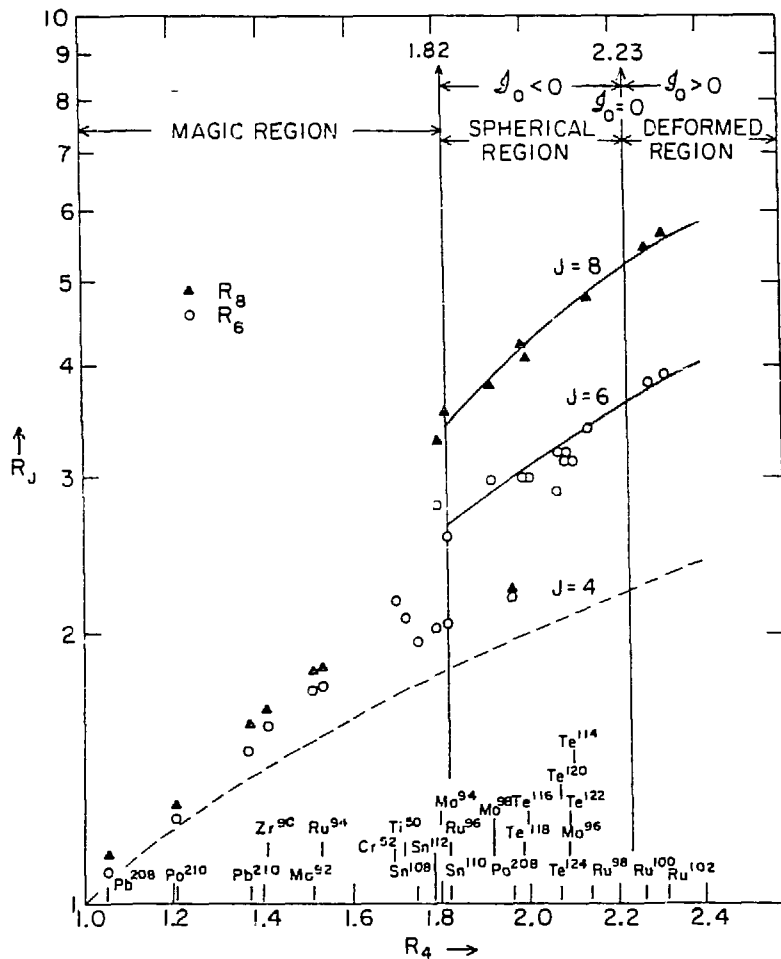


Fig. 3. Ratios R_6 and R_8 (logarithmic scale) as functions of R_4 for the magic and spherical regions. The solid curves are computed from eqs. 1 and 3. The dashed line indicates R_4 . In the magic zone the R_4 , R_6 , and R_8 values are almost degenerate. In ^{208}Po ($R_4 = 1.96$), "backbending" occurs already above the 4+ state.

This discovery "explained" the previously puzzling exception found for ^{208}Po (Fig. 3). The recently determined band¹¹⁾ for the semimagic nuclide ^{96}Pd was added to the figure.

The extension of the VMI equations to the magic limit made it possible to gain new insight into the relationship of nuclear moments of inertia to electric quadrupole moments—a relationship which had long resisted understanding: the rigid rotor concept had to be rejected early; it was first replaced by the "hydrodynamical model", which pictured the moment of inertia as being due to "irrotational motion". Neither \mathcal{J} nor Q was thought to change with increasing J . The introduction of BCS (pairing) theory into nuclear physics removed a major inconsistency, but could not explain the close correlation of \mathcal{J} with Q for a large range of nuclei which gradually emerged. The greatest difficulty arose when Q_{2+} values in "vibrational" nuclei [nuclei which have nearly vanishing values for $Q(J=0)$] were found to be considerably larger²⁾ than any existing microscopic theory could explain. However, now the definition¹⁾ for $\mathcal{J}_{02} \equiv \frac{1}{2}[(J=0) + \mathcal{J}(J=2)]$ could be deduced also for "vibrational" nuclei for which $\mathcal{J}(J=0)$ vanishes (see Fig. 5). (It may seem astonishing that the examples chosen coincide so closely with the best representatives of the three IBA I subgroups.) The increase of \mathcal{J} with J suggests—at least macroscopically—the explanation for the large Q_{2+} values. The empirical \mathcal{J}_{02} vs. Q_{02} correlation¹²⁾ (Fig. 6) led to two macroscopic models: 1) the alpha-dumbbell model for nuclei with ≤ 2 extra-shell nucleon pairs of one type (neutrons or protons) and 2) a two-fluid model (inertial fluid plus superfluid) for nuclei containing > 2 extra-shell neutron and proton pairs. This second model also explained the apparent A independence in the correlation, since it yields $\frac{\mathcal{J}}{Q^2} = \frac{A^{5/3}}{Z^2} \approx \text{const.}$ According to the hydrodynamic model, the A dependence was expected to be considerable ($\propto \frac{A^{1/3}}{Z^2}$). Figure 7 presents a linear plot of \mathcal{J} vs Q^2 . While the calculations show a deviation from the linear \mathcal{J} vs Q^2 relationship only for the heaviest nuclides, the experimental values deviate already for lighter (spontaneously fissioning) nuclei. This phenomenon may be due to a slight excess of protons over neutrons at the poles of these strongly

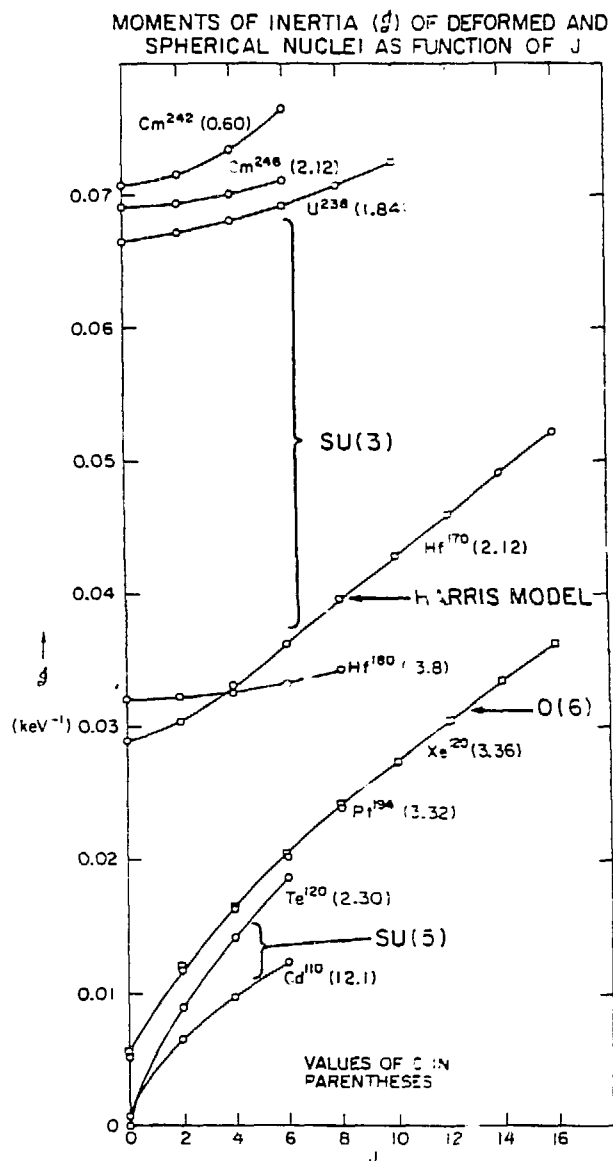


Fig. 5. Some representative examples of rotational bands (Hf^{180} , Hf^{170} , U^{238} , Cm^{242} , Cm^{248}), bands in transition nuclei (Xe^{120} , Pt^{194}), and "vibrational" bands (Cd^{110} , Te^{120}) are shown. Values for the stiffness parameters C in units of 10^6 keV^3 are given in parentheses. To this figure, first published in ref. 7, correspondences with subgroups of $\text{SU}(6)$ have now been added.

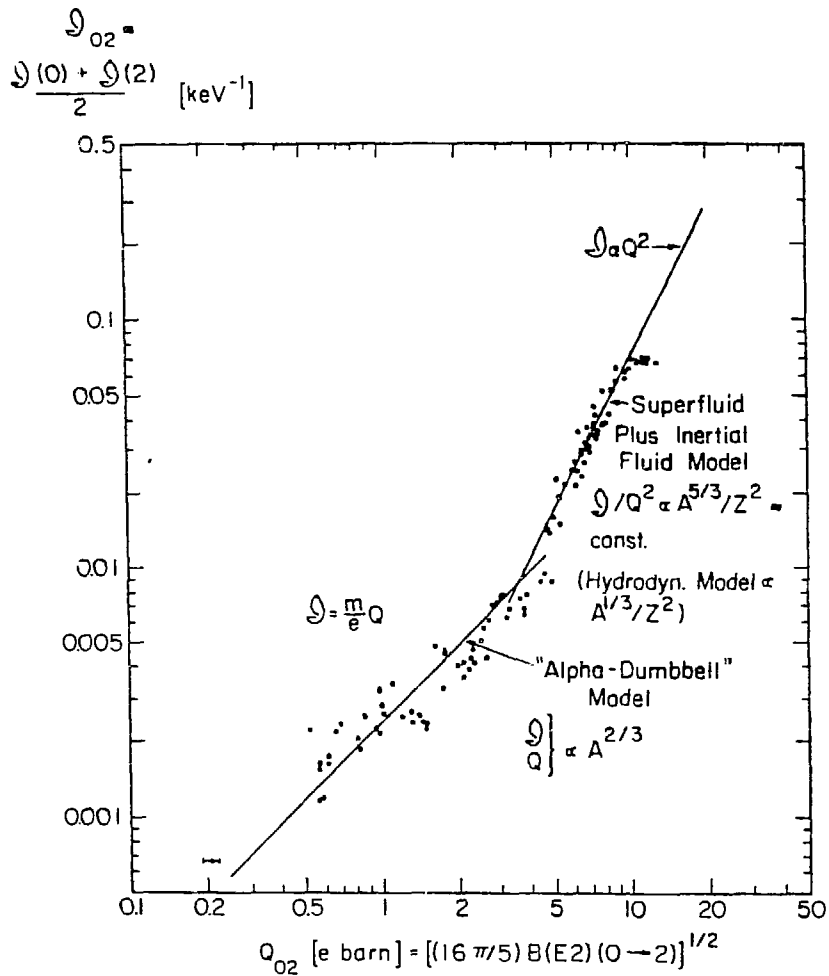


Fig. 6. Log log plot of the average moment of inertia $\mathcal{J}_{02} = \frac{\mathcal{J}(0) + \mathcal{J}(2)}{2}$ vs. the transition quadrupole moment Q_{02} . A linear part and a quadratic part can be clearly distinguished. The horizontal part for the highest \mathcal{J} - Q values refers to spontaneously fissioning actinides. The linear part is interpreted by the alpha-particle dumbbell model, the quadratic part by a macroscopic two-fluid model. (Figure taken from ref. 12.)

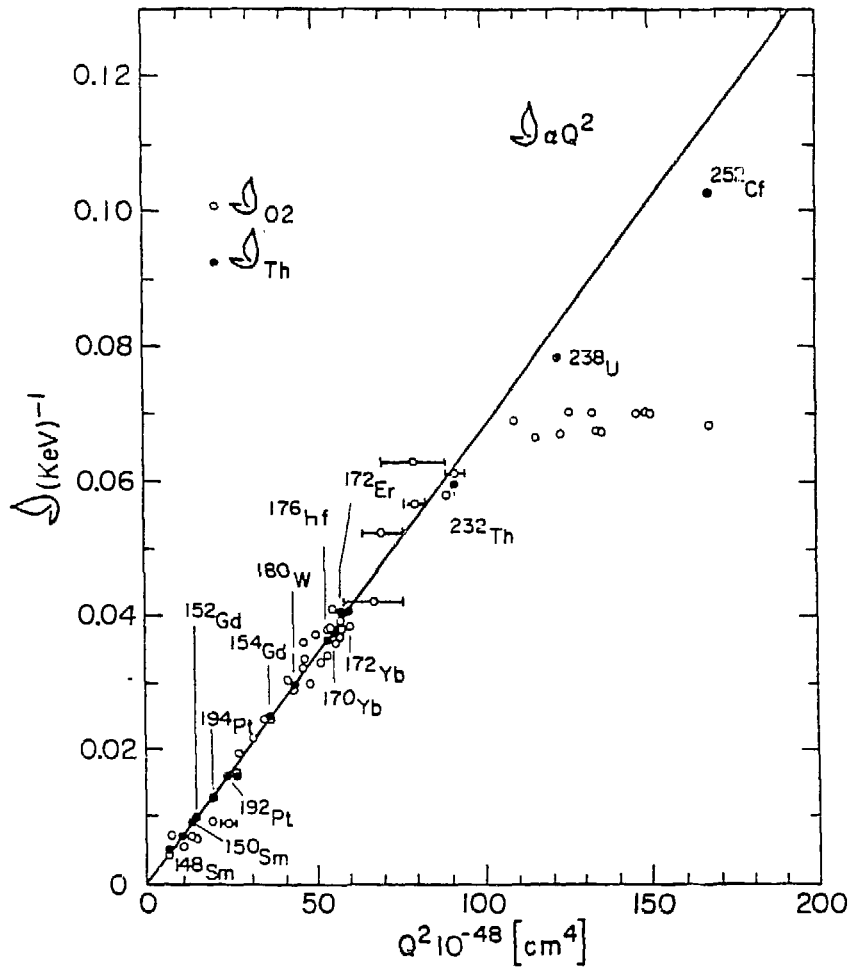


Fig. 7. Linear plot of α_{02} vs. Q_{02}^2 . Predictions from the two-fluid model are shown by solid circles, empirical values by open circles.

The straight line corresponds to $\alpha_{02} = 1/k^2 Q_{02}^2$, where $k = (39.4 \pm 2.6) \times 10^{-24} \text{ cm}^2(\text{keV})^{1/2}$. The Q_{02} values for the heaviest actinide nuclei increase by almost 50% while the α_{02} values remain approximately constant. (Figure first published in ref. 12.)

deformed nuclei. According to the hydrodynamic model, the A dependence was expected to be considerable. It should be noted that in both models the yrast bands are caused by "cranking", but the alpha-dumbbell configuration ("weak coupling" region) differs from that in the "strong coupling region".

The systematic study¹³⁾ of neutron deficient Pd and Ru nuclei ranging from ^{104}Pd ($N = 58$) to ^{96}Pd ($N = 50$) confirmed (and even exceeded) our expectations concerning the validity of VMI as shown in Fig. 8. This figure summarizes the comparison of the predictions of

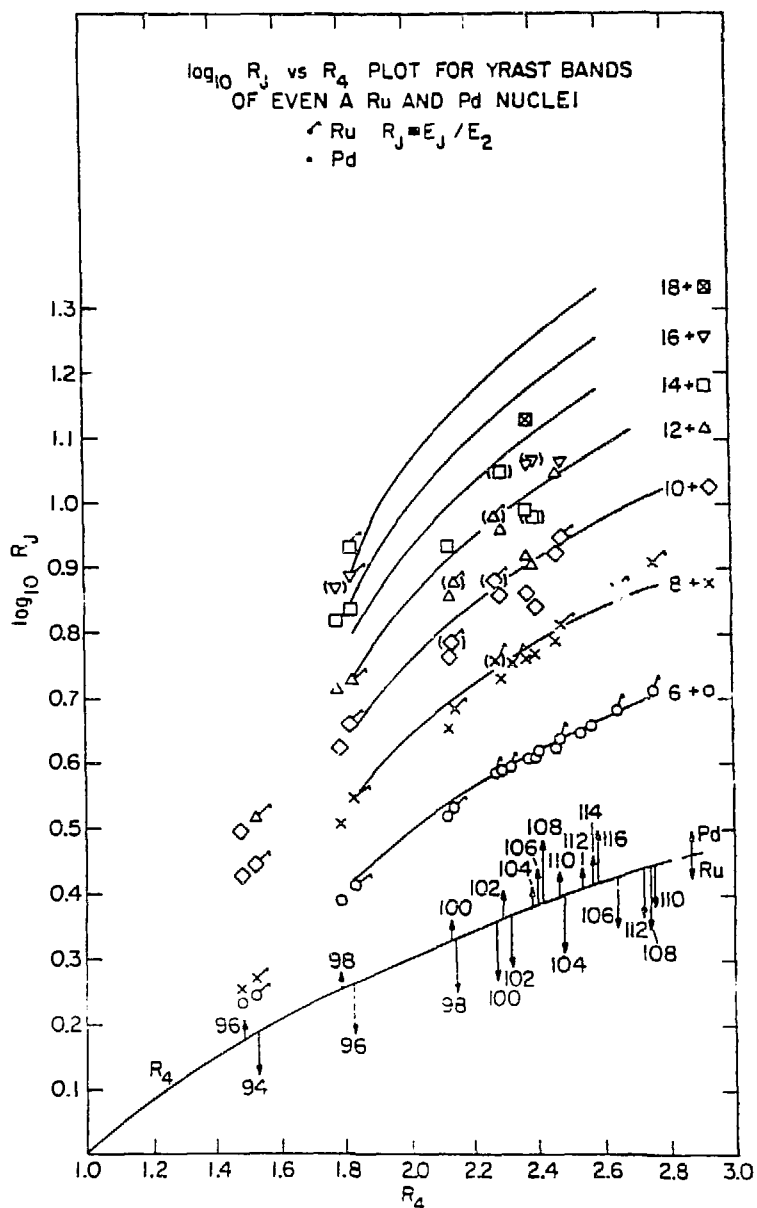


Fig. 8. A comparison of the even- A Pd ($96 \leq A \leq 116$) and Ru ($94 \leq A \leq 112$) yrast level energies with the energies predicted by the Variable Moment of Inertia (VMI) equations indicated by the solid curves. It is seen that the R_6 and R_8 values are in excellent agreement with VMI with the exception of pseudomagic ^{100}Pd . For ^{102}Pd , the agreement continues up to the 14^+ state and for ^{100}Ru up to the 12^+ state. For $^{104}, ^{106}\text{Pd}$, downwards deviations occur above the 8^+ level but in ^{110}Pd , the agreement is seen to persist to the 12^+ level.

the VMI equations for the even A Pd($96 \leq A \leq 116$) and Ru($94 \leq A \leq 112$) nuclides. The solid lines refer to $\log_{10} R_J$ vs R_4 as given by the VMI equations. The lowest curve shows R_4 ; the abscissa values for $Z = 46$ (Pd) isotopes are indicated by upward pointing arrows and for $Z = 44$ (Ru) isotopes by downward pointing arrows. The increase in R_4 near the middle of the neutron shell is larger for Ru (with six proton holes) than for Pd (with four holes). While the empirical R_6 and R_8 values are in excellent agreement with the VMI predictions, with the exception of pseudomagic $^{100}\text{Pd}^{10}$) (and of the R_8 values for the most deformed Ru nuclides which lie in a region of γ instability), backbending occurs in several of these nuclides above the 8+ state.

R_J values for the semimagic nuclei ^{96}Pd and ^{94}Ru lie in the "magic region", ($R_4 < 1.82$). Their yrast bands exhibit the expected decrease in the spacing of R_J values for $J \geq 4$ which is due to the fact that the 2+ states in these nuclei can only be populated by rearrangement (instead of cranking), such as the promotion of a pair of nucleons to a higher orbit. The ensuing lack of spherical symmetry makes cranking possible above this state.

Surprisingly, A. Klein who had contributed so much to the understanding of collective motions, stated¹⁴⁾ concerning the extension⁷⁾ of VMI: "Though a full and clear explanation has been provided for the possibility of mathematical extension of the original domain of definition of the formalism into the region of parameter space necessary for the extended applications, a physical understanding of this success remains elusive." Instead, he has proposed two generalizations of the anharmonic vibrator model, whose symmetry properties incorporate those of the subgroups of IBA I, and which result in three-parameter expressions for E_J . One of these is limited¹⁵⁾ by $R_4 = 2.0$, the other by $R_4 = 1.59$. Each one of them gives slightly better fits for certain yrast bands than the two parameter VMI expression. In another article, he has applied this approach to $^{98}, ^{100}, ^{102}\text{Pd}$ ¹⁶⁾.

This treatment appears to me to encounter the following difficulties:

- 1) The three "dynamic symmetries", corresponding to cases in

which the eigenvalue problem for the IBA boson Hamiltonian can be solved in analytic form, apply only to a few nuclei, and certainly not to the neutron deficient Pd nuclei.¹⁶⁾ Near the magic limit, as Talmi has pointed out, IBA I has to be replaced by the more complex IBA II approach.

2) A three-parameter formula has much less predictive value than one containing only 2 parameters since in many nuclei backbending takes place above $J = 8$. Moreover, the basic insight provided by the Mallmann observation, namely that the same mechanism holds for all even-even nuclei, is lost.

3) The endpoints¹⁵⁾ for the two versions proposed by Bonatsos and Klein, namely 1.59 and 2.0, contradict the evidence obtained from the spectra for the end point at 1.82.

REFERENCES

1. Mariscotti, J.A.J., Scharff-Goldhaber, G., and Buck, B Phys. Rev. B 178, 1864-87 (1969).
2. Scharff-Goldhaber, G., Dover, C., and Goodman, A.L., Ann. Rev. Nucl. Sci. 26, 239 (1976).
3. Scharff-Goldhaber, G., Nucl. Phys. A 347, 31 (1980).
4. Mallmann, C., Phys. Rev. Lett. 2, 507-9 (1959).
5. Das, T.K., Dreizler, R.M., and Klein, A., Phys. Rev. C 2, 632-38 (1970).
6. Ejiri, H., Ishihara, M., Sakai, M., Katori, K., and Inamura, T., J. Phys. Soc. Jpn 24, 1189 (1968).
7. Scharff-Goldhaber, G. and Goldhaber, A.S., Phys. Rev. Lett. 24, 1349-53 (1970).
8. Scharff-Goldhaber, G., Interacting Fermi-Bose Systems in Nuclei, F. Iachello ed., Plenum Publ. Corp., 263 (1981).
9. Scharff-Goldhaber, G. and Drsdn, M., "Transactions of the N.Y. Acad. of Sciences", Ser. II 40, 166 (1980).
10. Scharff-Goldhaber, G., J. Phys. G: Nucl Phys 5, 207 (1979), Corrigenda 6, 413 (1980).
11. Piel, W.F., Jr., Scharff-Goldhaber, G., Lister, C.J., and Varley, B.M., Phys. Rev C 28, 209 (1983).

12. Goldhaber, A.S. and Scharff-Goldhaber, G., Phys. Rev C 17, 1171 (1978).
13. Piel, W.F., Jr. and Sharff-Goldhaber, Phys. Rev. C 30 (No. 3), (1984) (in press).
14. Klein, A., Nucl. Phys. A 347, 3 (1980).
15. Bonatsos, D. and Klein, A., Phys. Rev. C 29, 1879 (1984).

DISCLAIMER

This report was prepared as an account of work sponsored by an agency of the United States Government. Neither the United States Government nor any agency thereof, nor any of their employees, makes any warranty, express or implied, or assumes any legal liability or responsibility for the accuracy, completeness, or usefulness of any information, apparatus, product, or process disclosed, or represents that its use would not infringe privately owned rights. Reference herein to any specific commercial product, process, or service by trade name, trademark, manufacturer, or otherwise does not necessarily constitute or imply its endorsement, recommendation, or favoring by the United States Government or any agency thereof. The views and opinions of authors expressed herein do not necessarily state or reflect those of the United States Government or any agency thereof.